Electrical Detection of Individual Magnetic Nanoparticles Encapsulated in Carbon Nanotubes

Jean-Pierre Cleuziou,[†,‡] Wolfgang Wernsdorfer,[†,*] Thierry Ondarçuhu,[‡] and Marc Monthioux[‡]

[†]Institut Néel, CNRS and Université J. Fourier, BP 166, 38042 Grenoble Cedex 9, France and [‡]Centre d'Elaboration des Matériaux et d'Etudes Structurales (CEMES), CNRS and Université de Toulouse, 29 rue Jeanne Marvig, 31055 Toulouse Cedex 4, France

ABSTRACT We report on low-temperature electrical transport measurements of single-walled carbon nanotubes (SWNTs) filled in their inner core with one-dimensional cobalt nanoparticles. The electrical transport properties of the hybrid devices are strongly sensitive to the magnetization reversal of isolated magnetic nanoparticles, resulting in strong hysteretic variations of the magnetoconductance. The magnetic anisotropy of a one-dimensional encapsulated cobalt nanoparticle is investigated, establishing an unusually strong dominating contribution of magnetic surface anisotropy.

KEYWORDS: hybrid carbon nanotubes · magnetic nanoparticles · molecular electronics · spintronics · nanomagnetism

The recent progress in the understanding of the electronic transport properties of individual nanometer-sized systems[1] opens the way to new spintronics devices, exploiting both the spin and charge of electrons in low-dimensional systems. In this context, carbon nanotubes are attracting a considerable interest in nanoscale electronics due to their rich transport properties, which have been used to implement devices ranging from high-performance field-effect transistors[2] to quantum dots[3] with well-defined spin and orbital structures.[4,5] Besides, the robust and tunable transport properties of nanotubes make them promising candidates as building blocks of hybrid spintronics devices aiming at the manipulation and the detection of electronic spins at the molecular scale.[6] For example, experiments on carbon nanotubes bridging ferromagnetic nanoelectrodes[7] have shown the spin-valve effect[8] and a strong gate dependence of magnetoresistance.[9−13]

The one-dimensional hollow nanostructure of SWNTs provides a unique model system for coupling to nanometer-sized magnetic objects (small magnetic clusters, metallofullerenes, molecular magnets, *etc.*) by surface functionalization or encapsulation.[6] An attractive way to achieve this goal consists of detecting the magnetic flux variations coming from the nanomagnet by using a carbon nanotube SQUID device.[14,15] The transport properties of a SWNT may be influenced by the nanomagnet owing to different mechanisms, permitting the readout of the magnetic spin states[16,17] as a sensitive local magnetometer. Other possibilities imply the indirect detection of the nanomagnet spin information through the carbon nanotube used as an accurate electrometer[18] in a single quantum dot regime to probe exchange-field interactions, dipolar couplings, or magneto-Coulomb effects[19,20] induced by the nanomagnet magnetic moment.

The encapsulation of magnetic transition metals inside SWNTs[21] has been realized experimentally[22−25] in the past few years and motivated many theoretical studies. Yang *et al.*[26] first proposed such metal-filled carbon nanotubes as promising spin-polarized transport devices with high spin polarization at the Fermi level.[27] On the other hand, there have been other recent studies on spin-polarized transport in nanotubes with single Fe and Co impurities.[28] The hybrid nanotube structures were predicted to exhibit substantial magnetic properties despite the fact that a hybridization between Co and C orbitals[29,30] showed clear signatures of resonant backscattering of one spin type (majority or minority spin). Both spin-dependent channels become quenched for several larger Co clusters (64 atoms in ref 29) randomly distributed along the nanotube, so that the spin polarization and total current are negligible.[29] Despite these theoretical investigations, very few electrical transport measurements of carbon nanotube magnetic hybrids are reported in the literature.[31,32]

* Address correspondence to wolfgang.wernsdorfer@grenoble.cnrs.fr.

Received for review January 4, 2011 and accepted February 11, 2011.

Published online February 23, 2011
10.1021/nn2000349

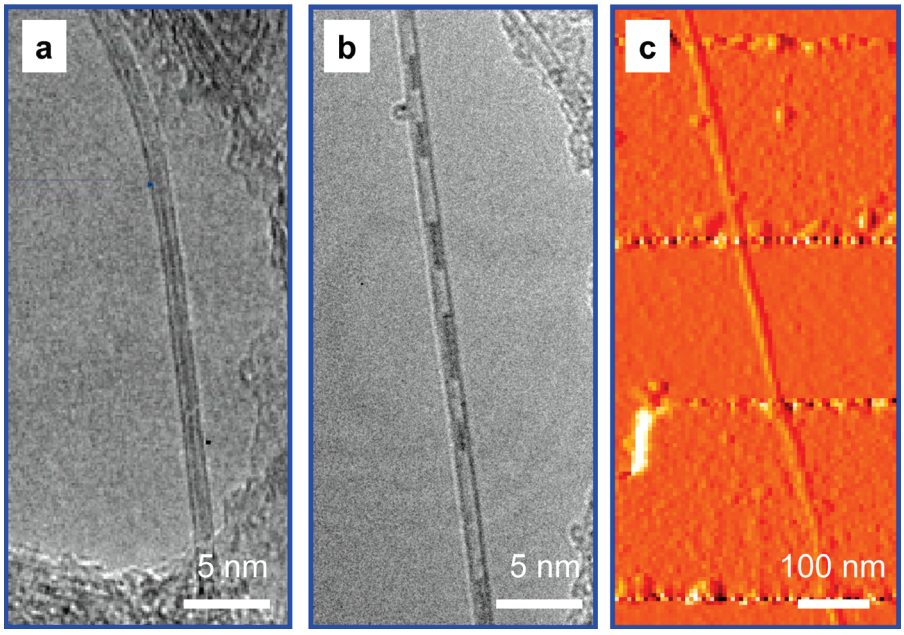

Figure 1. Images of cobalt-filled carbon nanotube samples. (a,b) TEM micrographs showing portions of individually filled SWNTs. The host material consists of continuous short nanowires of CoI_x (a), subsequently transformed in discrete elongated nanoparticles of Co (b) (see Methods section). (c) Atomic force microscope (AFM) image of a typical device, consisting of a bundle containing a few SWNTs ($d \sim 3.5$ nm) connected to Pd electrodes.

The first low-temperature electrical transport measurements of SWNTs partially filled with cobalt nanoparticles are presented. We show that the current−voltage characteristics of the hybrid device exhibit large magnetoconductance signals, which can be tuned in amplitude and sign by a gate voltage. We then demonstrate that these signals are directly related to the magnetization reversal of encapsulated nanoparticles of about 100 cobalt atoms.

RESULTS AND DISCUSSION

Hybrid Carbon Nanotube Devices. Figure 1a,b shows transmission electron microscope (TEM) images of the hybrid nanotubes. The SWNTs are first filled with CoI_2 nanowires with a length of up to 100 nm (Figure 1a) and then reduced in a second step under H_2 stream into cobalt nanoparticles inside the nanotube core (Figure 1b) (also see the Methods section). Most of the carbon nanotubes are not filled after the synthesis step, and only a fraction of them (~10%) are effectively partially filled with chains (Figure 1b) or isolated cobalt nanoclusters. The carbon shell creates low-dimensional[33] elongated well-defined particles constrained in a cross section inside the encapsulating carbon nanotubes[23,34] (Figure 1a, b). The particle lengths range from a few nanometers to 30−40 nm, with an average length of about 10 nm. The carbon nanotubes also provide an effective protection against oxidation of the ferromagnetic filling.

The resulting hybrid nanotubes are electrically connected with source and drain Pd electrodes on top of oxidized doped silicon substrates (serving as a backgate) (Figure 1c). Several devices were also fabricated on thin SiO_2 membranes compatible with TEM imaging (see Supporting Information) in order to observe directly the encapsulated material inside the connected nanotube used for transport measurements. Nevertheless, it was difficult to include the electrostatic gate needed for transport measurements, so we only describe here the results of devices in the standard geometry not compatible with TEM observations (Figure 1c).

Gate Dependence of Magnetoconductance. The transport of electrons in the nanotube hybrids is investigated by measuring the differential conductance $G = dI/dV$, as a function of the source-drain current I, gate voltage V_g, and applied magnetic field $\mu_0 H$. We report here measurements of a representative device that shows reproducible gate-controlled hysteretic loops of conductance. We have observed similar hysteretic behavior in eight comparable devices of cobalt-filled SWNTs. We report here measurements of small hybrid carbon nanotube bundles instead of single hybrid nanotubes where no such hysteretic features were observed.

Figure 2 shows single traces of G measured at a temperature of $T = 40$ mK as a function of V_g and $\mu_0 H$, by ramping the magnetic field at a constant rate from −2.5 to +2.5 T (sweep up) and subsequently decreasing from +2.5 to −2.5 T (sweep down). As the field is ramped, the conductance changes in a quasi-continuous manner until a sudden jump, ΔG_{sw}, is observed for both sweep directions (Figure 2a−c) at $\mu_0 H = \pm\mu_0 H_{sw} = \pm 1.28$ T (where the + and − signs correspond to the up and down sweep, respectively). This results in a pronounced hysteresis, which is symmetric with respect to

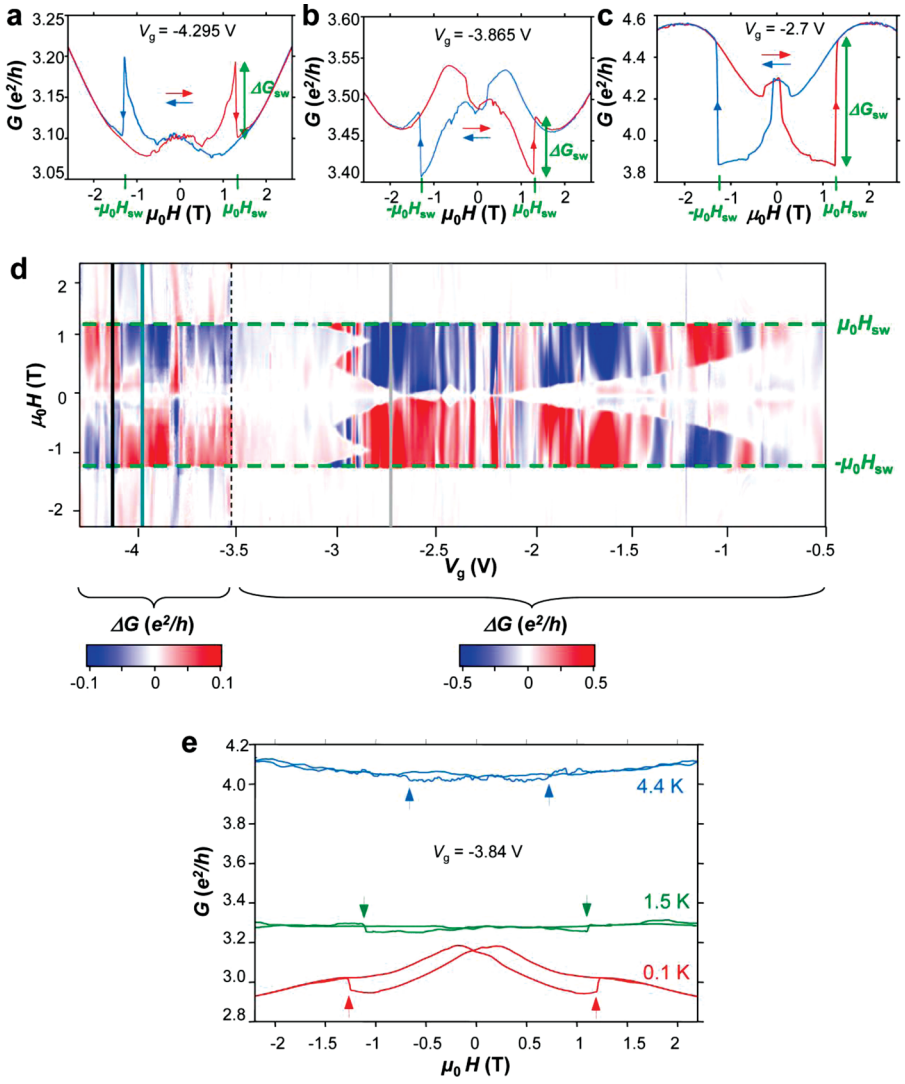

Figure 2. Conductance hysteresis loops of cobalt-filled carbon nanotubes. (a−c) Differential conductance d*I*/d*V* measured at temperature $T = 40$ mK as a function of in-plane magnetic field $\mu_0 H$ applied at an angle 25° with respect to the nanotube axis for different gate voltages. The red (blue) arrow in (a−c) indicates the up (down) magnetic field sweep direction. The strong dependence of both amplitude and sign of the jumps is observed in a large window of V_g in (d). We note the different conductance color scale for $V_g = -4.4$ to -3.5 V and for $V_g = -3.5$ to -0.5 V. (e) Temperature dependence of conductance hysteresis loops at $V_g = -3.84$ V.

$H = 0$. The discontinuities in G occur at the same field ($\mu_0 H_{sw} = \pm 1.28$ T), but the sign and amplitude of the conductance jumps depend strongly on V_g (for both up and downfield sweep directions). For example, at $V_g = -4.295$ V (Figure 2a), G changes abruptly at $\mu_0 H_{sw}$ from $G = 3.2e^2/h$ to a lower conductance of $G = 3.1e^2/h$, yielding to a negative jump $\Delta G_{sw} \approx -0.1e^2/h$ ($\Delta G_{sw}/G \approx -3\%$). In contrast, at $V_g = -3.865$ V (Figure 2b), G jumps from $G = 3.41e^2/h$ to $G = 3.48e^2/h$, yielding to a positive jump $\Delta G_{sw} \approx +0.07e^2/h$ ($\Delta G_{sw}/G \approx +2\%$). The magnitude of ΔG_{sw} depends also strongly on V_g. For example, at $V_g = -2.7$ V (Figure 2c), its magnitude is much more important and reaches $\Delta G_{sw} \approx +0.6e^2/h$ ($\Delta G_{sw}/G \approx +15.3\%$). We also note that the conductance maximum at $H = 0$ ($G \approx 4.3e^2/h$) exceeds the maximum conductance ($4e^2/h$) carried by a single nanotube, suggesting that our sample is a bundle of a few SWNTs in parallel. The full set of data measured for a large V_g window ranging from -4.4 to -0.5 V is presented in Figure 2d, where the hysteresis of conductance (the difference of conductance between up and downfield sweeps) is color-plotted as a function of V_g and $\mu_0 H$. We observe that $\mu_0 H_{sw}$ is independent of V_g and that there is no magnetic hysteresis at $H = 0$. The strong gate dependence of both contrast and magnitude of the conductance jumps is seen for many different V_g (Figure 2d). The hysteresis temperature dependence of one conductance jump is presented in Figure 2e ($V_g = -3.84$ V). The magnitudes of ΔG and H_{sw} decrease rapidly as the temperature is raised from 50 mK, while the overall conductance increases. The conductance jump amplitude is strongly correlated to the device conductance and amplified at lower temperatures where the onset of Coulomb blockade reduces the overall conductance. Above 4.4 K, the overall

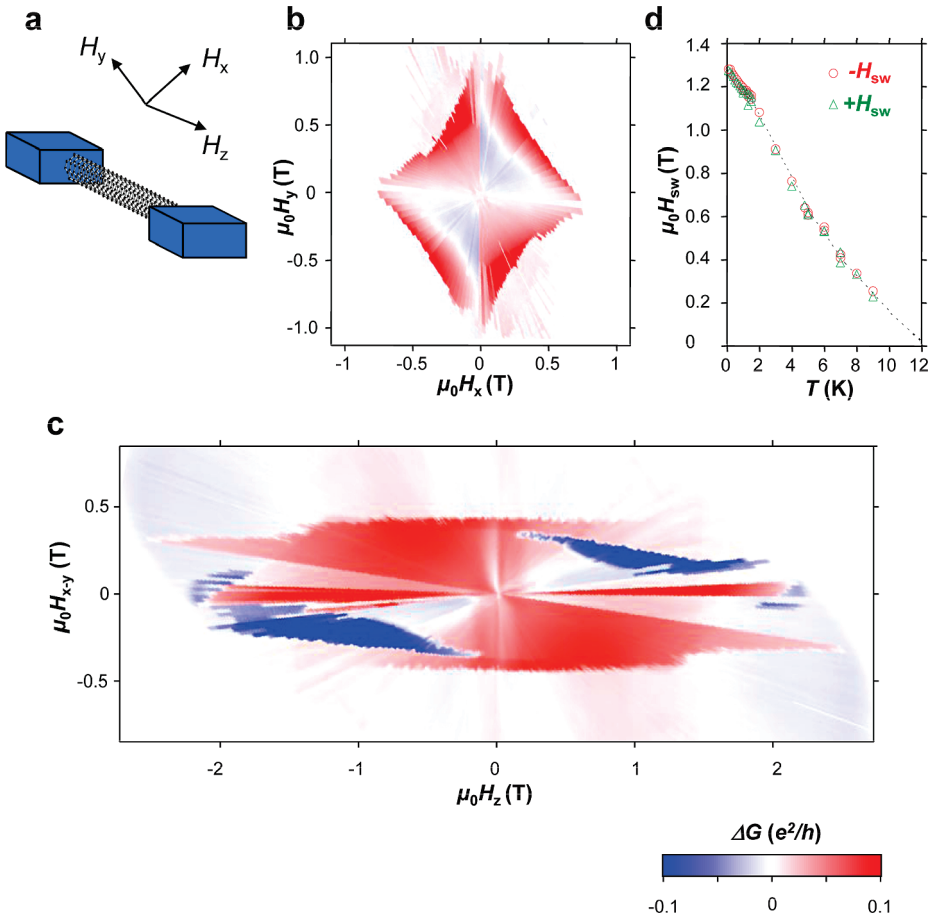

Figure 3. Angular and temperature dependences of the switching field. (a) Schematic representation of the hybrid nanotube junction and definition of field direction: *z*-axis is parallel to the nanotube axis, while the *x*- and *y*-axes are perpendicular to the junction axis. (b,c) Color scale plot of the differential conductance d*I*/d*V* at temperature $T = 40$ mK in a H_x-H_y plane, perpendicular to the nanotube axis (b) and in a plane $H_{x-y}-H_z$ belonging to the junction plane (c). (d) Temperature dependence of the switching field H_{sw}. An extrapolation of H_{sw} to 0 gives the blocking temperature $T_B \approx 12$ K.

conductance increases up to $4.1e^2/h$, suggesting that electronic transport is carried by another nanotube, becoming conducting as Coulomb interactions are reduced.

The conductance hysteresis is very reproducible over many V_g and $\mu_0 H$ sweeps and is superposed to other conductance variations[35] depending on both $\mu_0 H$ and V_g. The SWNTs before the filling procedure also show this quasi-continuous dependence of the conductance with magnetic field (see Supporting Information). Nevertheless, the abrupt conductance jumps and hysteresis depicted in Figure 2 are only observed in cobalt-filled nanotubes. In the following, we show that these jumps are correlated to the magnetization reversal of single encapsulated nanoparticles.

Magnetization Reversal Detection of Single Magnetic Nanoparticle. In order to demonstrate that conductance jumps (Figure 2) are due to the magnetization reversal of a single encapsulated cobalt nanoparticle, we study their dependence as a function of the applied field direction[36] and temperature.[37] The sample is measured by sweeping the magnetic field according to the directions defined with respect to the nanotube axis in Figure 3a. Figure 3b,c shows the hysteresis of the conductance as a function of a magnetic field applied in the plane perpendicular to the nanotube axis (H_x-H_y plane) and in the plane containing the nanotube axis ($H_{x-y}-H_z$ plane), respectively.

The switching field H_{sw} (at which the conductance jump occurs) changes mostly continuously as a function of the field direction and follows the well-known Stoner–Wohlfarth model[38] that describes the magnetization reversal of one single nanoparticle by uniform rotation of the magnetization. Indeed, a detailed study of the angular dependence of H_{sw} shows that Figure 3b,c represents two cross sections of the Stoner–Wohlfarth astroid, where H_x, H_y, and H_z are the field directions along the easy, medium hard, and hard axes, respectively. The well-defined shape of the astroid proves without any doubt that the sharp conductance jumps of Figure 2 are attributed to the magnetization reversal of only one single encapsulated cobalt nanoparticle with a preferential magnetization orientation with respect to the host carbon nanotube axis. Figure 3d presents the temperature dependence of the switching field.

H_{sw} decreases as the temperature is raised, and at the blocking temperature of $T_B \approx 12$ K, the thermal energy is sufficient to reverse the magnetization at $H = 0$, that is, H_{sw} becomes 0. Knowing the magnetic anisotropy along the medium hard axis (Figure 3b), we can estimate the number of atoms[37] $N \approx 200$. When considering the nearest neighboring distance between two cobalt atoms in bulk (2.5 Å), we deduce the length of a related 1 nm large cylindrical particle to be $l \approx 15 \pm 5$ nm, which is very consistent with nanoparticle sizes typically observed (Figure 1b).

Strong Uniaxial Anisotropy of One-Dimensional Encapsulated Cobalt Nanoparticles. The two cross sections of the Stoner−Wohlfarth astroid of Figure 3 show a strong dominating uniaxial anisotropy with an easy axis of magnetization perpendicular to the nanotube axis in all samples. It establishes that the strong surface magnetocrystalline anisotropy[38] overcomes the shape anisotropy and causes an alignment of the magnetization perpendicular to the nanoparticle surface.[39−41] This behavior is different than that of larger cylindrical ferromagnetic particles (∼10−50 nm in diameter) encapsulated in multiwalled carbon nanotubes[42] where the dominating shape anisotropy forces the magnetization to be along the nanotube axis. The surface magnetocrystalline anisotropy, coming from the broken symmetry of the cobalt crystalline structure at the interface with the encapsulating carbon nanotube, is greatly enhanced in our particles due to the large fraction of cobalt atoms at the surface. It arises from the low dimensionality and the high aspect ratio of nanoparticles when encapsulated in SWNTs. H_{sw} measured along the hard magnetization axis (*i.e.*, the carbon nanotube axis) is very large ($\mu_0 H_{sw} > 2$ T in Figure 3c) and corresponds to a strong anisotropy energy density about 1 order of magnitude higher than typical anisotropies reported on few nanometer-sized cobalt clusters.[38,43] The observed anisotropy suggests also that cobalt atoms arrange preferentially in a fcc-type structure.

Magneto-Coulomb Effect and Spin-Polarized Transport. After demonstrating the electrical detection of the magnetization reversal of separated encapsulated cobalt nanoparticles, we now discuss the magnetoconductance origin in our devices. We have considered two main different schemes to explain the origin of the magnetoconductance in carbon nanotubes filled with cobalt (Figure 4). The two main possibilities imply the electronic transport to occur either directly through the magnetic cobalt nanostructures encapsulated in a single carbon shell (Figure 4a) or in an empty-like nanotube in close proximity to the cobalt nanoparticles encapsulated in a parallel nonconducting tube (Figure 4b).

The situation depicted in Figure 4a is favorable to the injection of strong spin-polarized currents from cobalt-filled portions. The detection of spin-polarized currents needs at least two different magnetic

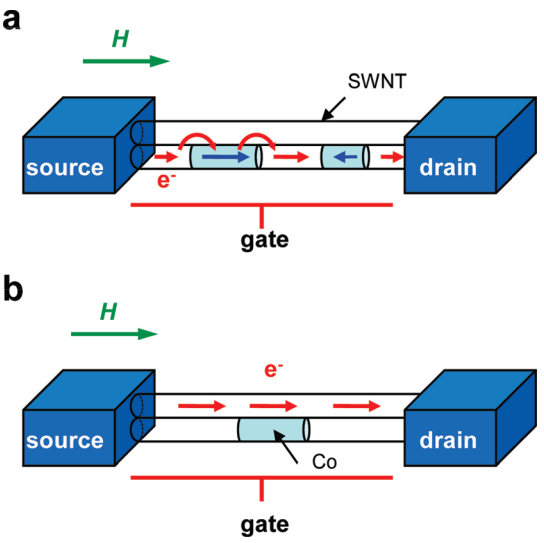

Figure 4. Spin-dependent transport mechanisms in cobalt-filled carbon nanotubes. Schematic representation of a small bundle of partially filled SWNTs. (a) Electrons flow directly through the filled nanotube portions connected to unfilled ones where a spin-polarized current may be injected and detected owing to the spin-valve effect. (b) Electronic transport mainly occurs through one nanotube well-connected and coupled locally in parallel to a single cobalt nanoparticle. One single nanoparticle is expected to induce a significant magneto-Coulomb effect.

nanoparticles, one called "analyzer", the other one "polarizer", separated by an empty nanotube section. In this case, the device would operate as a nanometer-sized spin valve where a magnetoconductance difference is expected for parallel and antiparallel orientations of the two encapsulated ferromagnets.[7−9] This picture agrees well with the theoretical predictions of Yang *et al.*[26−28] and others who calculated very high spin polarization in SWNTs filled with cobalt.[26−28]

The other possibility, represented in Figure 4b, implies that SWNTs filled with small portions of cobalt are nonconducting[29] and that current should be mainly carried by a nonmagnetic unfilled nanotube in the small bundle.[44] According to recent *ab initio* transport calculations of SWNTs partially filled with cobalt clusters, a strong reduction of the total conductance is expected due to the quenching of the spin conductance channels.[29,30] In this scheme, the encapsulated nanoclusters are thus weakly interacting electronically to the electronic transport. Since nanotubes are sensitive to single electron charging effects, a magneto-Coulomb effect[45,46] may account for large gate-dependent magnetoconductance. This effect principle is based on the electrostatic transfer of the nanoparticle Zeeman energy, accumulated under an applied magnetic field,[47] to an effective change of the nanotube charge state (a more detailed description is given in Supporting Information).

We now discuss our data in more detail and compare them to the two schemes of Figure 4. The single hysteretic switching reported in Figures 2 and 3, with a

constant switching field for all gate voltages, shows that only one nanoparticle is responsible for a large magnetoconductance signal. It thus excludes spin-valve operation where at least two nanoparticles would be necessary for injection and detection of spin-polarized currents (see previous discussion). Besides, the rapid decrease of the magnetoconductance hysteretic features from the very low temperature regime (Figure 2e) does not seem to be compatible with spin polarization effects that should be conserved up to the blocking temperature ($T_B \sim 12$ K). The strong increase of magnetoconductance at the onset of Coulomb interactions below a few Kelvin is expected for magneto-Coulomb effect. Indeed, the charging energy of the device has to be strong enough to observe such an effect. At temperatures higher than 4 K, charging energy vanishes dramatically, so that magneto-Coulomb effect cannot play a role and hysteretic magnetoconductance features disappear. The magnetoconductance amplitude is clearly correlated to the overall device conductance and increases as Coulomb blockade is relevant at very low temperatures (Figure 2e). The strong amplification of the conductance jumps for a precise gate voltage range (from $V_g = -3$ to -0.7 V in Figure 2c,d) highlights again the important role of single electron charging effects on the device magnetoconductance. In addition, the gate dependence of both sign and amplitude of the hysteretic magnetoconductance is predicted in the frame of magneto-Coulomb effect (see Supporting Information). A full investigation of the mechanism cannot be studied here, due to the irregularity of the color-plotted pattern of Figure 2d. This behavior has been recurrently reported in low-temperature transport measurements of carbon nanotubes and arises, for example, from the influence of defects induced by imperfections in the SWNT structure or adsorbed residues produced by device processing.[48] In our case, the encapsulation of cobalt clusters accounts for a significant additional source of disorder that prevents the observation of a single quantum dot. Disorder and few conducting nanotubes in parallel prevent a simple correlation between magnetoconductance and conductance slope at zero field (see Supporting Information).

CONCLUSION

In conclusion, we have reported the strong sensitivity of carbon nanotube transport properties to the magnetization reversal of separated encapsulated clusters of only a few hundreds of cobalt atoms. We also demonstrated that cobalt nanoparticles preserve their magnetic properties when encapsulated in SWNTs, with unusual enhanced surface magnetic anisotropy causing the magnetization to be perpendicular to the host nanotube axis. The mechanism responsible for the gate-dependent magnetoconductance is more favorably explained by a magneto-Coulomb effect. Nevertheless, spin polarization effects are not completely excluded in this system and may pave the way to very high-performance spin-polarized transistors based on nanosized ferromagnets encapsulated in carbon nanotubes. Further theoretical work and improvements in device processing are required for the full investigation of filled carbon nanotube potential. More generally, we strongly believe that carbon nanotube devices offer a powerful way to readout the magnetic properties of functionalized single nanomagnets.

METHODS

Synthesis of One-Dimensional Cobalt Nanoparticles Encapsulated in Carbon Nanotubes. Empty SWNTs (from Nanocarblab) were synthesized by the electrical arc method using nickel−yttrium-doped graphite anode and purified by multistage procedure consisting of concentrated nitric acid and controlled annealing in air. The SWNTs were then filled in high yield by the capillary wetting technique that consists of the impregnation of SWNTs with molten cobalt iodide[49] (CoI_2, Aldrich, 99.9%) at 550 °C. The mixture was held at this temperature for 24 h, after which it was allowed to cool to room temperature at a slow rate (0.1 °C min^{-1}) to induce good crystallization of the incorporated material. The exterior halide, not incorporated into the tubes, was washed and filtered with ethanol. These treatments led to a partial filling of the SWNTs with CoI_x, as checked by TEM observations (Figure 1a). To transform CoI_x (Figure 1a) into Co nanoparticles (Figure 1b), hybrid nanotubes were annealed in H_2/Ar atmosphere[50] (45 mL min^{-1} of H_2 with 70 mL min^{-1} of Ar) at 400 °C for 24 h.

Device Fabrication. To build the cobalt-filled carbon nanotube device of Figure 1c, we started from a degenerately n-doped silicon substrate used as a back-gate, on top of which a 350 nm thick SiO_2 layer was thermally grown. A few droplets of the hybrid nanotubes dispersed in 1,2-dichloroethane (DCE) were placed on the substrate and washed with isopropyl alcohol (IPA). The junctions were made from straight sections of carbon nanotubes located by AFM imaging, on top of which 50 nm thick metallic Pd electrodes were deposited by aligned electron beam lithography and standard lift-off technique. Only devices with resistance below 50 kΩ and no significant gate effect at room temperature were selected for this study. It was not possible to image the cobalt filling inside the junctions by AFM, TEM, or magnetic force microscopy (MFM). The devices were therefore measured without knowing if the filled segments of carbon nanotubes lay between the electrodes. We fabricated about 300 devices, using mainly individual SWNTs ($d \sim 1-1.5$ nm) and also thin bundles ($d < 4$ nm) in order to increase the cobalt filling probability in the junction.

Acknowledgment. This work was partially supported by the CNRS ACI NOCIEL, ANR QuSpins, ANR-08-NANO-002 MolNanoSpin, the ERC Advanced Grant MolNanoSpin 226558, and European MolSpinQIP programs. Clean room processes were supported by the CNRS RTB program using the technological facilities of the Laboratory for Analysis and Architecture of Systems (University of Toulouse, France). We thank F. Carcenac, E. Eyraud, L. Levy, H. Bouchiat, J. M. Broto, C. Vieu, and X. Blase for valuable contributions and helpful discussions.

Supporting Information Available: Additional experimental details and transport measurements. This material is available free of charge *via* the Internet at http://pubs.acs.org.

REFERENCES AND NOTES

1. Roch, N.; Florens, S.; Bouchiat, V.; Wersndorfer, W.; Balestro, F. Quantum Phase Transition in Single-Molecule Quantum Dot. *Nature* **2008,** *453*, 633–637.
2. Javey, A.; Guo, J.; Wang, Q.; Lundstrom, M.; Dai, H. Ballistic Carbon Nanotube Field Effect Transistors. *Nature* **2003,** *424*, 654–657.
3. Tans, S. J.; Devoret, M. H.; Dal, H.; Thess, A.; Smalley, R. E.; Geerligs, L. J.; Dekker, C. Individual Single-Wall Carbon Nanotubes as Quantum Wires. *Nature* **1997,** *386*, 474–477.
4. Minot, E. D.; Yaish, Y.; Sazonova, V.; McEuen, P. L. Determination of Electron Orbital Magnetic Moments in Carbon Nanotubes. *Nature* **2004,** *428*, 536–539.
5. Jarillo-Herrero, P.; Kong, J.; van der Zant, H. S. J.; Dekker, C.; Kouwenhoven, L. P.; De Franceschi, S. Kondo Effect in Carbon Nanotubes. *Nature* **2005,** *434*, 484–488.
6. Bogani, L.; Wernsdorfer, W. Molecular Spintronics Using Single-Molecule Magnets. *Nat. Mater.* **2008,** *7*, 179–186.
7. Tsukagoshi, K.; Alphenaar, B. W.; Ago, H. Coherent Transport of Electron Spin in a Ferromagnetically Contacted Carbon Nanotube. *Nature* **1999,** *401*, 572–574.
8. Hueso, L. E.; Pruneda, J. M.; Ferrari, V.; Burnell, G.; Valdes-Herrera, J. P.; Simons, B. D.; Littlewood, P. B.; Artacho, E.; Fert, A.; Mathur, N. D. Transformation of Spin Information into Large Electrical Signals Using Carbon Nanotubes. *Nature* **2007,** *445*, 410–413.
9. Sahoo, S.; Kontos, T.; Furer, J.; Hoffmann, C.; Gräber, M.; Cottet, A.; Schönenberger, C. Electric Field Control of Spin Transport. *Nat. Phys.* **2005,** *1*, 99.
10. Hauptmann, J. R.; Paaske, J.; Lindelof., P. E. Electric-Field-Controlled Spin Reversal in a Quantum Dot with Ferromagnetic Contacts. *Nat. Phys.* **2008,** *4*, 373–376.
11. Man, H. T.; Wever, I. J. W.; Morpugo, A. F. Spin-Dependent Quantum Interference in Single-Wall Carbon Nanotubes with Ferromagnetic Contacts. *Phys. Rev. B.* **2006,** *73*, 241401(R).
12. Merchant, C. A.; Marković, N. Electrically Tunable Spin Polarization in a Carbon-Nanotube Spin Diode. *Phys. Rev. Lett.* **2008,** *100*, 156601.
13. Cottet, A.; Kontos, T.; Sahoo, S.; Man, H. T.; Choi, M.-S.; Belzig, W.; Bruder, C.; Morpurgo, A. F.; Schönenberger, C. Nanospintronics with Carbon Nanotubes. *Semicond. Sci. Technol.* **2006,** *21*, S78–S95.
14. Chen, R. J.; Bangsaruntip, S.; Drouvalakis, K. A.; Kam, N. W. S.; Shim, M.; Li, Y. Noncovalent Functionalization of Carbon Nanotubes for Highly Specific Electronic Biosensors. *Proc. Natl. Acad. Sci. U.S.A.* **2003,** *100*, 4984–4989.
15. Bogani, L.; Danieli, C.; Biavardi, E.; Dalcanale, E.; Bendiab, N.; Wernsdorfer, W.; Cornia, A. Single-Molecule-Magnet Carbon-Nanotube Hybrids. *Angew. Chem., Int. Ed.* **2008,** *48*, 746–750.
16. Cleuziou, J. P.; Wernsdorfer, W.; Bouchiat, V.; Ondarcuhu, T.; Monthioux, M. Carbon Nanotube Superconducting Quantum Interference Device. *Nat. Nanotechnol.* **2006,** *1*, 53.
17. Cleuziou, J. P.; Wernsdorfer, W.; Andergassen, S.; Florens, S.; Bouchiat, V.; Ondarçuhu, M.; Monthioux, M. Gate-Tuned High Frequency Response of Carbon Nanotube Josephson Junctions. *Phys. Rev. Lett.* **2007,** *99*, 117001.
18. Gruneis, A.; Esplandiu, M. J.; Garcia-Sanchez, D.; Bachtold, A. Detecting Individual Electrons Using a Carbon Nanotube Field-Effect Transistor. *Nano Lett.* **2007,** *7*, 3766–3769.
19. Ono, K.; Shimada, H.; Ootuka, Y. Enhanced Magnetic Valve Effect and Magneto-Coulomb Oscillations in Ferromagnetic Single Electron Transistor. *J. Phys. Soc. Jpn.* **1997,** *66*, 1261–1264.
20. Shimada, H.; Ono, K.; Ootuka, Y. Magneto-Coulomb Oscillations in Ferromagnetic Single-Electron Transistors. *J. Phys. Soc. Jpn.* **1998,** *67*, 1359–1370.
21. Monthioux, M.; Flahaut, E.; Cleuziou, J. P. Hybrid Carbon Nanotubes: Strategy, Progress and Perspectives. *J. Mater. Res.* **2006,** *21*, 2774–2793.
22. Zoican Loebick, C.; Majewska, M.; Ren, F.; Haller, G. L.; Pfefferle, L. D. Fabrication of Discrete Nanosized Cobalt Particles Encapsulated Inside Single-Walled Carbon Nanotubes. *J. Phys. Chem. C* **2010,** *114*, 11092–11097.
23. Borowiak-Palen, E.; Mendoza, E.; Bachmatiuk, A.; Ruemmeli, M. H.; Gemming, T.; Nogues, J.; Skumryev, V.; Kalenczuk, R. J.; Pichler, T.; Silva, S. R. P. Iron Filled Single-Wall Carbon Nanotubes—A Novel Ferromagnetic Medium. *Chem. Phys. Lett.* **2006,** *421*, 129–133.
24. Li, Y. F.; Hatakeyama, R.; Kaneko, T.; Izumida, T.; Okada, T.; Kato, T. Electrical Properties of Ferromagnetic Semiconducting Single-Walled Carbon Nanotubes. *Appl. Phys. Lett.* **2006,** *89*, 083117.
25. Li, Y. F.; Hatakeyama, R.; Kaneko, T.; Okada, T. Nano Sized Magnetic Particles with Diameters Less than 1 nm Encapsulated in Single-Walled Carbon Nanotubes. *Jpn. J. Appl. Phys.* **2006,** *45*, L428.
26. Yang, C. K.; Zhao, J.; Lu., J. P. Magnetism of Transition-Metal/Carbon-Nanotube Hybrid Structures. *Phys. Rev. Lett.* **2003,** *90*, 257203.
27. Kang, Y. J.; Choi, J.; Moon, C.-Y.; Chang, K. J. Electronic and Magnetic Properties of Single-Wall Carbon Nanotubes Filled with Iron Atoms. *Phys. Rev. B* **2005,** *71*, 115441.
28. Jo, C.; Lee, J. Magnetism of Fe, Co, and Ni Nanowires Encapsulated in Carbon Nanotubes. *J. Magn. Magn. Mater.* **2008,** *320*, 3256–3260.
29. Blase, X.; Margine, E. R. Resonant Spin-Filtering in Cobalt Decorated Nanotubes. *Appl. Phys. Lett.* **2009,** *94*, 173103.
30. Fürst, J. A.; Brandbyge, M.; Jauho, A. P.; Stokbro, K. *Ab Initio* Study of Spin-Dependent Transport in Carbon Nanotubes with Iron and Vanadium Adatoms. *Phys. Rev. B* **2008,** *78*, 195405.
31. Soldano, C.; Kar, S.; Talapatra, S.; Nayak, S.; Ajayan, P. M. Detection of Nanoscale Magnetic Activity Using Single Carbon Nanotube. *Nano Lett.* **2008,** *8*, 4498–4505.
32. Li, Y.; Kaneko, T.; Ogawa, T.; Takahashi, M.; Hatakeyama, R. Novel Properties of Single-Walled Carbon Nanotubes with Encapsulated Magnetic Atoms. *Jpn. J. Appl. Phys.* **2008,** *47*, 2048–2055.
33. Sloan, J.; Luzzi, D. E.; Kirkland, A. I.; Hutchison, J. L.; Green, M. L. H. Imaging and Characterization of Molecules and One-Dimensional Crystals Formed within Carbon Nanotubes. *MRS Bull.* **2004,** *29*, 265–271.
34. Satishkumar, B. C.; Taubert, A.; Luzzi., D. E. Filling Single-Wall Carbon Nanotubes with d- and f-Metal Chloride and Metal Nanowires. *J. Nanosci. Nanotechnol.* **2003,** *3*, 159–163.
35. Deshpande, V. V.; Bockrath, M. The One-Dimensional Wigner Crystal in Carbon Nanotubes. *Nat. Phys.* **2008,** *4*, 314–318.
36. Bonet, E.; Wernsdorfer, W.; Barbara, B.; Benoit, A.; Mailly, D.; Thiaville, A. Three Dimensional Magnetization Reversal Measurements in Nanoparticles. *Phys. Rev. Lett.* **1999,** *83*, 4188–4191.
37. Wernsdorfer, W.; Bonet Orozco, E.; Hasselbach, K.; Benoît, A.; Barbara, B.; Demoncy, N.; Loiseau, A.; Boivin, D.; Pascard, H.; Mailly, D. Experimental Evidence of the Neel-Brown Model of Magnetization Reversal. *Phys. Rev. Lett.* **1997,** *78*, 1791–1794.
38. Jamet, M.; Wernsdorfer, W.; Thirion, C.; Mailly, D.; Dupuis, V.; Mélinon, P. Magnetic Anisotropy of a Single Cobalt Nanocluster. *Phys. Rev. Lett.* **2001,** *86*, 4676.
39. Allenspach, R.; Stampanoni, M.; Bischof, A. Magnetic Domains in Thin Epitaxial Co/Au(111) Films. *Phys. Rev. Lett.* **1990,** *65*, 3344–3347.
40. Speckmann, M.; Oepen, H. P.; Ibach, H. Magnetic Domain Structures in Ultrathin Co/Au (111): On the Influence of Film Morphology. *Phys. Rev. Lett.* **1995,** *75*, 2035–2038.
41. Dreyer, M.; Kleiber, M.; Wadas, A.; Wiesendanger, R. Composition-Driven Change of the Magnetic Anisotropy of Ultrathin Co/Au(111) Films Studied by Means of Magnetic-Force Microscopy in Ultrahigh Vaccum. *Phys. Rev. B* **1999,** *59*, 4273–4278.

42. Kozhuharova, R.; Ritschel, M.; Elefant, D.; Graff, A.; Leonhardt, A.; Moench, I.; Muehl, T.; Groudeva-Zotova, S.; Schneider, C. M. Well-Aligned Co-Filled Carbon Nanotubes: Preparation and Magnetic Properties. *Appl. Surf. Sci.* **2004,** *238*, 355–359.
43. Guéron, S.; Deshmukh, M. M.; Myers, E. B.; Ralph, D. C. Tunneling *via* Individual Electronic States in Ferromagnetic Nanoparticles. *Phys. Rev. Lett.* **1999,** *83*, 4148–4151.
44. Zwanenburg, F. A.; van der Mast, D. W.; Heersche, H. B.; Bakkers, E. P. A.; Kouwenhoven, L. P. Electric Field Control of Magnetoresistance in InP Nanowires with Ferromagnetic Contacts. *Nano Lett.* **2009,** *9*, 2704–2709.
45. Bernand-Mantel, A.; Seneor, P.; Bouzehouane, K.; Fusil, S.; Deranlot, C.; Petroff, F.; Fert, A. Anisotropic Magneto-Coulomb Effects and Magnetic Single-Electron-Transistor Action in a Single Nanoparticle. *Nat. Phys.* **2009,** *5*, 920–924.
46. van der Molen, S.; Tombros, J.; van Wees, N.; Magneto-Coulomb, B. J. Effect in Spin-Valve Devices. *Phys. Rev. B* **2006,** *73*, 220406(R).
47. Tombros, N.; van der Molen, S. J.; van Wees, B. J. Separating Spin and Charge Transport in Single-Wall Carbon Nanotubes. *Phys. Rev. B* **2006,** *73*, 233403.
48. Bockrath, M.; Liang, W.; Bozovic, D.; Hafner, J. H.; Lieber, C. M.; Tinkham, M.; Park, H. Resonant Electron Scattering by Defects in Single-Walled Carbon Nanotubes. *Science* **2001,** *291*, 283–285.
49. Philp, P.; Sloan, J.; Kirkland, A. I.; Meyer, R. R.; Friedrichs, S.; Hutchison, J. L.; Green, M. L. H. An Encapsulated Helical One-Dimensional Cobalt Iodide Nanostructure. *Nat. Mater.* **2003,** *2*, 788–791.
50. Costa, P. M. F. J.; Sloan, J.; Rutherford, T.; Green, M. L. H. Encapsulation of Re_xO_y Clusters within Single-Walled Carbon Nanotubes and Their in Tubulo Reduction and Sintering to Re Metal. *Chem. Mater.* **2005,** *17*, 6579–6582.